Long-Range Transport of Water Channelized through the Southern Subtropical Jet

Eliane Larroza, Philippe Keckhut, Jean-Luc Baray, Walter Nakaema, Hélène Vérèmes, Eduardo Landulfo, Davide Dionisi, Sergey Khaykin, François Ravetta

atmosphere

MDPI

Article

Long-Range Transport of Water Channelized through the Southern Subtropical Jet

Eliane G. Larroza [1,2,*], Philippe Keckhut [2,*], Jean-Luc Baray [3], Walter M. Nakaema [4], Hélène Vérèmes [5], Eduardo Landulfo [1], Davide Dionisi [6], Sergey Khaykin [7] and François Ravetta [2]

1 CLA, IPEN/CNEN-SP, Center for Lasers and Applications, Av. Prof. Lineu Prestes, 2242, São Paulo 05508-000, Brazil; elandulf@ipen.br
2 LATMOS/IPSL, UMR8190, UPMC Univ. Paris 06 Sorbonne Universités, UVSQ, CNRS, 4 Place Jussieu, 75252 Paris, France; Francois.ravetta@latmos.ipsl.fr
3 OPGC/LaMP, Laboratoire de Météorologie Physique, UMR 6016 Université Clermont Auvergne/CNRS, 63178 Aubière CEDEX, France; J.L.Baray@opgc.fr
4 IFSP, Instituto Federal de Educação, Ciência e Tecnologia de São Paulo, Rua Pedro Vicente, 625, Canindé, São Paulo 01109-010, Brazil; walter.nakaema@ifsp.edu.br
5 LACy, Laboratoire de l'Atmosphère et des Cyclones, UMR8105, Université de La Réunion, Météo-France, CNRS, 97490 Saint-Denis de La Réunion, France; helene.veremes@univ-reunion.fr
6 ISAC-CNR, Instituto di Scienze dell'Atmosfera e del Clima, Consiglio Nazionale delle Ricerche, 00133 Roma, Italy; d.dionisi@isac.cnr.it
7 LATMOS/IPSL, UVSQ, Université Paris-Saclay, UPMC Univ. Paris 06, CNRS, 11 Boulevard d'Alembert, 78280 Guyancourt, France; sergey.khaykin@latmos.ipsl.fr
* Correspondence: Eliane.Larroza@latmos.ipsl.fr or eliane.larroza@ipen.br (E.G.L.); Philippe.Keckhut@latmos.ipsl.fr (P.K.); Tel.: +55-(11)-3133-9361 (E.G.L.); +33-(0)-1-80-28-52-50 (P.K.)

Received: 8 August 2018; Accepted: 15 September 2018; Published: 25 September 2018

Abstract: In this study, an air mass (containing a cirrus cloud) was detected by light detection and ranging (lidar) above São Paulo (Brazil) in June 2007 and tracked around the globe, thanks to Lagrangian calculations as well as ground-based and satellite observations. Cloud-Aerosol Lidar and Infrared Pathfinder Satellite Observation (CALIPSO) data were also used to provide locations of occurrence of cirrus around the globe and extract their respective macro physical parameters (altitude and temperature). An analysis of the air mass history based on Lagrangian trajectories reveals that water coming from the Equator is channelized through the southern subtropical jet for weeks. In this case, the back-trajectories showed that the cirrus cloud detected at São Paulo was a mixture of air masses from two different locations: (1) the active convective area located around the Equator, with transport into the upper troposphere that promotes cirrus cloud formation; and (2) the South Pacific Ocean, with transport that follows the subtropical jet stream (STJ). Air masses coming from equatorial convective regions are trapped by the jet, which contributes to maintaining the lifetime of the cirrus cloud for a few days. The cloud disappears near the African continent, due to a southern excursion and warmer temperatures, then reappears and is detected again by the lidar system in São Paulo after 12 days. The observed cloud is located at a similar altitude, revealing that sedimentation is small or compensated by radiative uplift.

Keywords: cirrus; water vapor; subtropical jet

1. Introduction

In the lower stratosphere, water vapor plays a key role in the radiation budget [1]. Moreover, upper tropospheric cirrus clouds are highly dependent on local temperature and water vapor

concentration, which also has a significant impact on the radiative balance [2]. In the tropics, convection plays a dominant role in setting the humidity of the tropical tropopause layer (TTL), and coupled with cold tropical tropopause temperatures, controls the amount of water vapor entering into the stratosphere, (above 380 to 400 K potential temperature) in the ascending branch of the Brewer–Dobson circulation [3]. The convective injection of water in the lower stratosphere by an anvil cirrus cloud has been observed remotely from aircraft and satellite imagery [4–6]. According to the literature, two potential mechanisms of formation has been identified: the gravity wave breaking downstream of the overshooting top [4], and the turbulent mixing and advection downwind of the overshooting top itself [7]. In the tropics, water vapor is transported from the troposphere to the stratosphere through the TTL, which extends vertically over several kilometers from around 14 to 19 km [8]. The amount of moist air and the mechanisms that control air transport through the TTL, such as convective overshooting and other issues [3,9], are still not entirely understood. Global climate models (GCM) have difficulties simulating water vapor density and cirrus cloud occurrence in the TTL and the lower stratosphere, revealing large differences between themselves depending on the parametrization used [10–12].

Over São Paulo, continuous cirrus cloud observations by MSP (Metropolitan city of São Paulo) light detection and ranging (lidar) reveal that the clouds' origins are either coming along the subtropical jet stream (STJ), or from equatorial convective areas around the Gulf of Mexico going south along the Andes, or even a mixture of both types of cloud origins [13]. These observations suggest some potential preferred routes and the existence of permanent moist air over the sub-tropical jet. Long duration balloons measuring the cloud vertical structure, temperature, and water vapor as planned by the National Centre for Space Studies (CNES) [14] during the Strateole 2 campaign would be well adapted to address such issues.

While a Lagrangian approach appears to be well-adapted to study the evolution and maintenance of cirrus in the upper troposphere [9], another approach consists in sampling air masses by several ground-based instruments, as well as by Cloud-Aerosol Lidar and Infrared Pathfinder Satellite Observation (CALIPSO) when its lidar ground-path crosses the cirrus trajectories. Space lidar systems on sun-synchronous polar orbits have the ability to frequently cross the quasi-horizontal trajectory of tropical air masses; however, the time matching is a major difficulty to provide multiple sampling. The methodology proposed here is similar to Dionisi et al. [15], in which two ground-based lidar systems in Europe have allowed the quantification of cirrus crystals' sedimentation, in a different geographical context.

We have tracked a cirrus case study that is representative to cirrus frequently observed over São Paulo, in order to evaluate how such an approach can allow a better description of water transport in the upper troposphere/lower stratosphere (UTLS) region. This study can be considered as a benchmark experience for preparing future balloon campaigns and a feasibility study of Lagrangian cirrus tracking, using two ground-based lidars at a similar latitude and one space-based lidar.

The ground-based lidar observations used in this study are described in Section 2, while the transport of air masses associated with this case is discussed in Section 3. The observations of the space lidar CALIOP (Cloud–Aerosol Lidar with Orthogonal Polarization) on CALIPSO matching best air mass trajectories are presented and discussed in Section 5. The conclusions can be found in Section 6.

2. Cirrus Clouds Observations

2.1. Ground-Based Lidars

2.1.1. MSP-Lidar at São Paulo

Cirrus clouds have been frequently observed at São Paulo (23°33′ S, 46°44′ W), by MSP-lidar measurements since 2004 [13]. This lidar is a single-wavelength backscatter system pointing vertically toward the zenith and operating in the coaxial mode, and uses an Nd:YAG pulsed laser source at the wavelength of 532 nm for cirrus detection, with a fixed repetition rate of 20 Hz. The temporal resolution of measurements is ~2 min and the vertical resolution is 15 m. More details about the system

used in this work can be found in Larroza et al. [13], and the performance description can be found in Landulfo et al. [16].

2.1.2. Rayleigh Lidar at Réunion Island

Lidar operations at Réunion Island started in 1993 on the university campus located in Saint-Denis (21° S, 55°22′ E). This site was equipped with various instruments for atmospheric measurements: tropospheric and stratospheric ozone lidars, Raman water vapor lidar, wind lidar, spectro-radiometers, and in-situ gas and aerosol sensors. This lidar is also based on Nd:YAG pulsed laser source at the wavelength of 532 nm. Detail descriptions of improvements made upon this system have been detailed by Baray et al. [17]. The Rayleigh lidar had specific channels for cirrus and polarized channels [18]. In 2012, most of the lidar equipment was moved from Saint-Denis to the Maïdo altitude site [19].

2.1.3. Methodology of Cirrus Cloud Detection

Cirrus cloud retrieval presented in this study is based on the methodology described in Larroza et al. [13]. The total backscattering coefficient β_{total} can be obtained using a reference altitude of 30 km, where the backscattering contribution is mainly due to air molecules, aerosol scattering being negligible. The β_{total} is further used to calculate the apparent scattering ratio (SR_{app}), which is defined as the ratio of the total (molecular and particle) backscatter coefficient divided by the molecular backscatter coefficient $\beta_{Rayleigh}$. $\beta_{Rayleigh}$ can be estimated from a dry air density profile, retrieved from the conventional radiosonde observation profile [20].

2.1.4. Cirrus Observations from São Paulo and Réunion Island (June 2007)

Based on the availability of many measurements from the MSP-lidar, and the a-priori representativeness of that type of cirrus over São Paulo, we have selected the cloud observed on 1 June 2007, which had a double layer structure (Figure 1). This cirrus cloud extended over 2.5 km from 13.5 km to 16 km altitudes. The cloud top is located around the potential temperature of 380 K, close to the TTL. On 12 June, a cirrus cloud was again reported over São Paulo with a similar vertical extension, but at a lower altitude. The associated potential temperature of 355 K corresponded to mid-latitude tropopause. The scattering ratio was smaller (around 8) with a thin pic up to 18 (Figure 1).

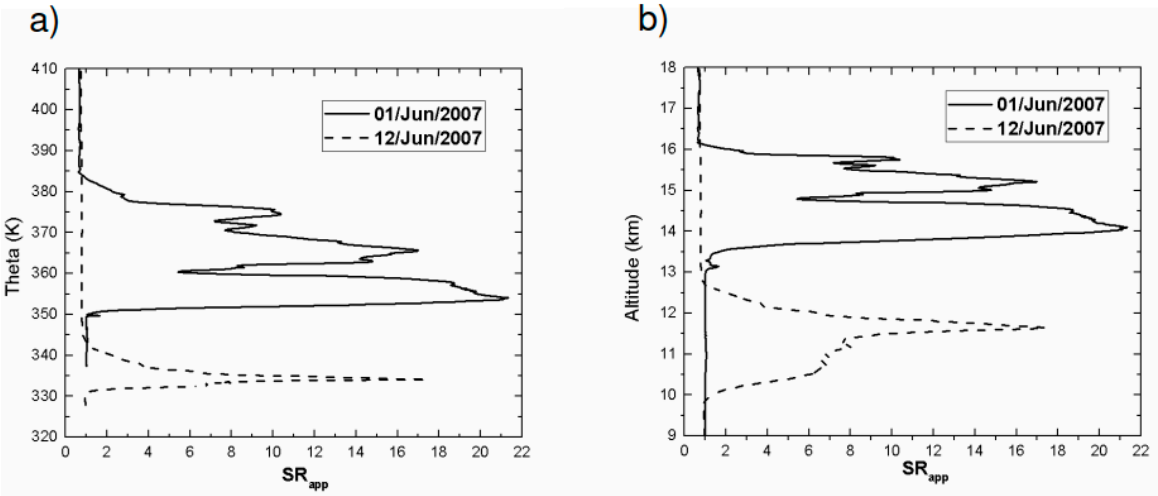

Figure 1. SR_{app} profiles on 1 June (solid line) and 12 June (dashed line) 2007 derived from the São Paulo lidar, according to the potential temperature (from local radiosounding) (**a**) and the corresponding altitudes (**b**).

The lidar observation over Saint-Denis at Réunion island on 4 June 2007 matched the time and trajectory of the air mass previously observed by São Paulo on 1 June, exhibiting a thin cirrus layer

from 12 to 14 km, with a scattering ratio of up to 20 (shown as an inset in Figure 2) and a thick cirrus at 10 km of about 3 km thickness (Figure 2).

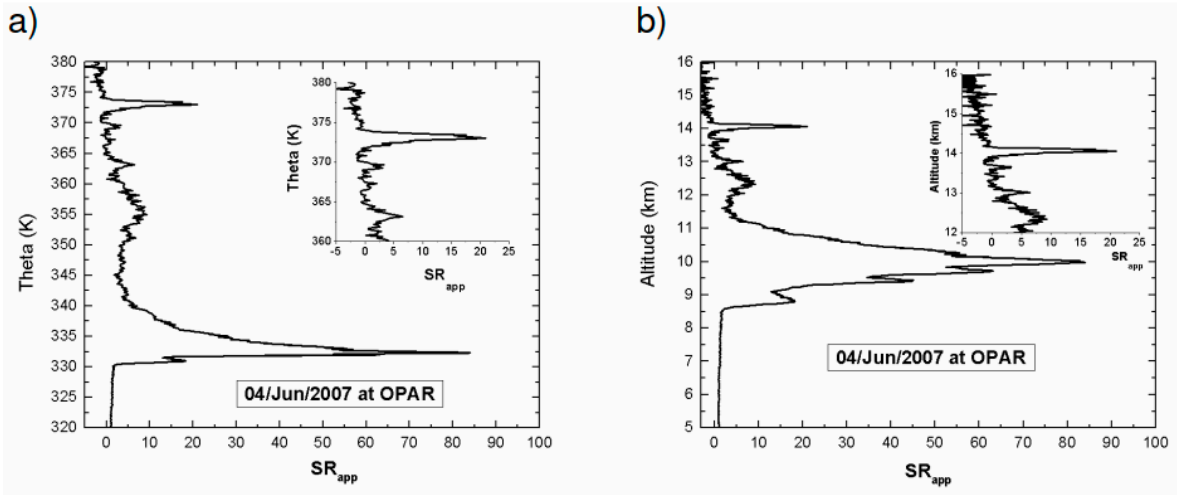

Figure 2. SR_{app} profile observed by the lidar at Maïdo on 4 June 2007 at ~16h 50 UTC, according to the potential temperature (from ECWMF-ERA-Interim (Dataset of global atmospheric reanalysis stated as European Centre for Medium-Range Weather Forecasts Re—Analysis continued since 1979)) (**a**) and the corresponding altitudes (**b**).

2.2. CALIPSO Plataform

CALIPSO is a joint National Aeronautics and Space Administration (NASA)-CNES satellite mission, designed to provide insight into the role of aerosols and clouds in the climate system [21]. This system consists of several onboard instruments with distinct functions. For example, the CALIOP is designed to collect vertical profiles of elastic backscatter at two wavelengths (1064 nm and 532 nm) from a near-nadir viewing geometry during both day and night phases of the orbit.

In the CALIOP operational algorithm [21], the layers are detected using the level 1, 532-nm total attenuated backscatter, β_{532}, [22] at a horizontal resolution of 1 km and a vertical resolution of 60 m [23], which are further classified as clouds or aerosols [24].

The CALIOP temperature data analyzed in this study are derived from the GEOS-5 (Goddard Earth Observing System) model and provided by GMAO (Global Modeling Assimilation Office). More details can be found in Anselmo et al. [25].

3. Transport of Cirrus Air Masses

3.1. Trajectory Analyses

The sampling strategy to characterize the origin of cirrus clouds detected initially by MSP-lidar over São Paulo, and its subsequent tracking, has allowed observation of the signature of the water vapor in the upper troposphere of a subtropical region. In order to determine the origin of cirrus, as a well as to follow air masses in maintaining these clouds, we performed trajectory analyses using the LACYTRAJ code (Lagrangian trajectory code from Laboratoire de l'Atmosphère et des Cyclones (Université de la Réunion)) [26]. LACYTRAJ calculations are based on three-dimensional winds from the ECMWF (European Centre for Medium Range Weather Forecasts) ERA-Interim daily global reanalysis [27], with a 1-degree horizontal resolution (latitude-longitude), and 37 vertical pressure levels. Each backward and forward cluster of trajectories is calculated every 15 min for 312 h, with a starting vertical level corresponding to lidar cirrus clouds observations. In this work, we also interpolated atmospheric parameters in time and space in order to study the temporal evolution of atmospheric conditions inside and near the edges.

3.2. Source of Moist Air

Ensemble backward trajectories were initialized on 1 June 2007 at 18:00 UTC until 20 May 2007 at 18:00 UTC (UTC—Universal Time Coordinated is a coordinate time scale, maintained by the Bureau International des Poids et Mesures (BIPM)) for the mean level of the cirrus cloud at 14.5 km observed by MSP-lidar (Figure 1). The back-trajectories (Figure 3a) indicate a mix of air masses coming from the Equator at 13–14 km, lifted up above the Caribbean Sea at a high convective region from the ground, with equatorial air masses already at 14 km.

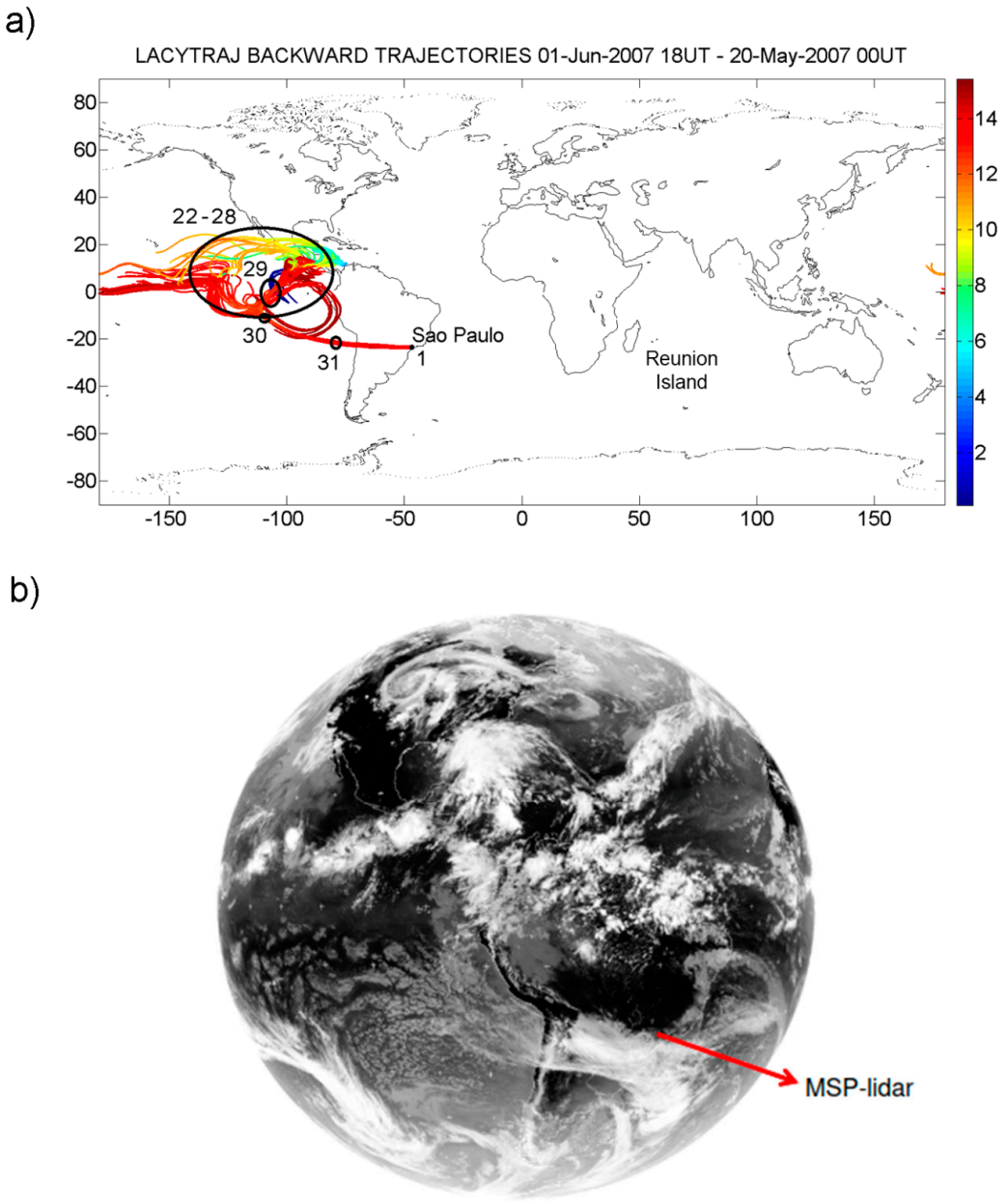

Figure 3. (**a**) Backward trajectories corresponding to the cirrus cloud detected by metropolitan city of São Paulo (MSP)-lidar on 1 June 2007 at São Paulo. Colors indicate the air masses altitudes (in km), and the numbers indicate the day of May–June 2007 corresponding to the location of the air masses. (**b**) METEOSAT (METEOSAT—Meteorological Satellite (METEOSAT) series of satellites are geostationary meteorological satellites operated by EUMETSAT (European Organization for the Exploitation of Meteorological Satellites) under the Meteosat Transition Program (MTP) an the Meteosat Second Generation (MSG) program) InfraRed (IR) at 18 UTC on 1 June 2007.

3.3. Transport from São Paulo

The air masses corresponding to the lidar observations on 1 June were guided by the STJ and transported at nearly the same latitude (observations between 10° S and 40° S) during 12 days after reaching São Paulo again, as indicated by the LACYTRAJ forward trajectories (Figure 4a). The METEOSAT IR image (Figure 4b) shows the presence of clouds superimposed on the STJ on that day.

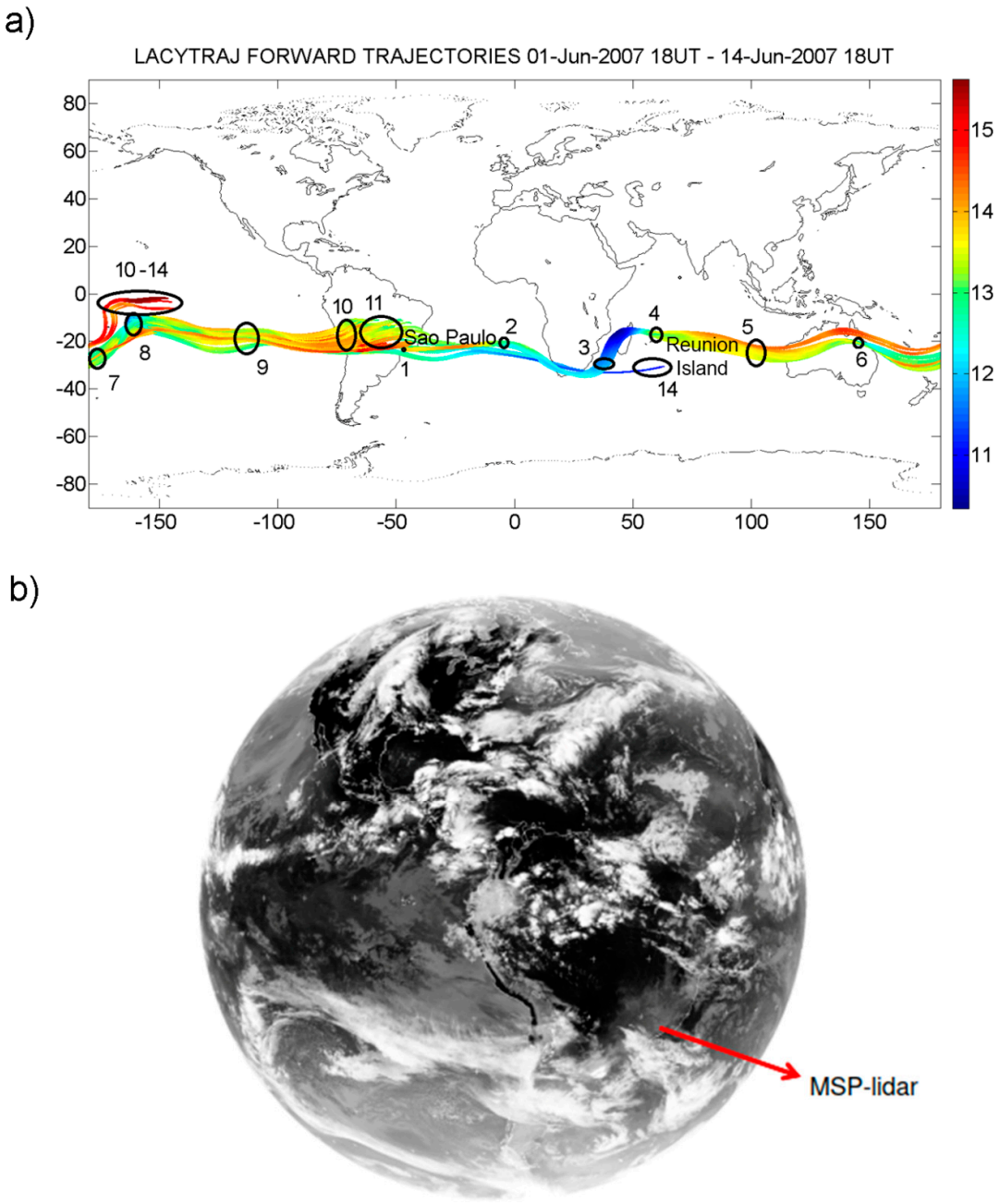

Figure 4. (**a**) Forward trajectories corresponding to the cirrus cloud detected by MSP-lidar on 1 June 2007 at São Paulo. Colors indicate the air mass altitudes (in km), and the numbers indicate the day of June 2007, corresponding to the location of the air masses. (**b**) METEOSAT InfraRed (IR) at 18 UTC on 12 June 2007, showing cirrus clouds transported by the jet stream in the Pacific before reaching again São Paulo.

The trajectories indicate that air masses are shifted southward when crossing the African continent, which is associated with an altitude decrease (Figure 5a), then follow the isentropic level (Figure 5b), and then experience lower temperatures (Figure 5c). Cirrus cloud between 12 and 14 km still exist (Figure 2), but are considerably reduced in thickness compared to the São Paulo observations (Figure 1), probably due to warmer temperatures, according to the temperature evaluation illustrated on Figure 5 that indicates an increase of around 25 K.

The global wind field at 200 hPa in the southern hemisphere indicates a permanent intense flow in the latitude band of 20–40° S. This is consistent with a monthly climatology of the daily STJ position over the 30-year period (1979–2008) for the southern hemisphere in the vicinity of South America, which is between 100° and 30° W and 10° and 40° S as presented by Zimmermann [28]. In addition, according to Escobar [29], this STJ can be found in generally above 13 km at the same latitude range, although it can vary seasonally between 30° and 35° S.

However, these flows are sometimes perturbed, allowing larger meridional transport [30]. At the beginning of 1 June 2007, South America was mainly under the influence of air flow coming from Caribbean golf (Figure 3a).

A one-year climatological study shows that the occurrence of cirrus is significant in the vicinity of the tropics, particularly in the western Pacific war pool area, the equatorial sections of western Africa and South America, and to a somewhat lesser extent the linear feature associated with the inter-tropical convergence zone (ITCZ) that tends to tie these areas together [31]. This phenomenon is linked to the presence of the ITCZ, formed by the convergence of hot and humid air masses from the tropics and carried by the trade winds. Thus, the general occurrence of cirrus clouds is well correlated with the locations of deep convective clouds in the tropical region [32].

The air masses probed by the lidar are mainly coming from the ITCZ, as shown in Figure 3. Convection is highly active in the ITCZ, bringing water vapor from the low to upper troposphere, converting it into anvil ice clouds and ice crystals, which are transported isentropically, down to higher latitudes.

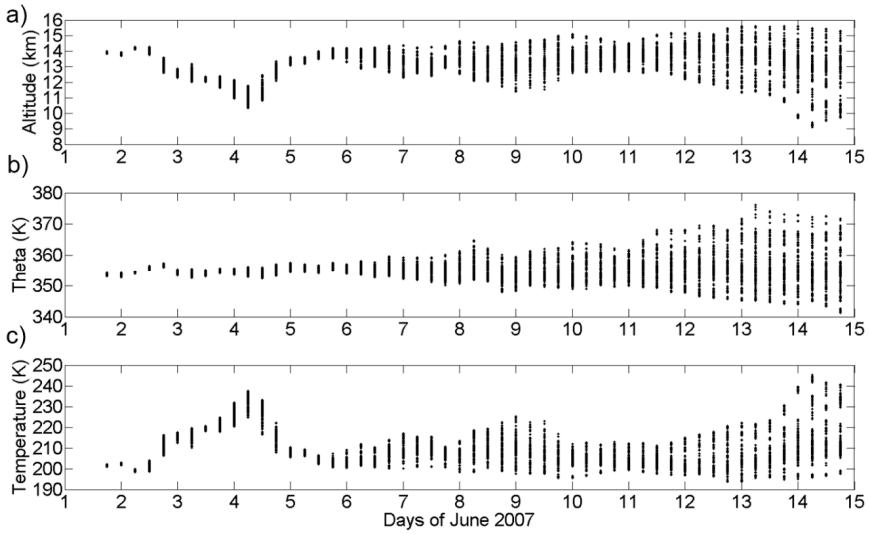

Figure 5. Temporal evolution of (**a**) altitude (in km, deduced from pressure level) and thermodynamic parameters; (**b**) theta (in K); and (**c**) temperature, interpolated on LACYTRAJ forward trajectories points during 15 days (1 to 15 June 2007).

This case illustrates that air masses reaching the STJ are strongly deflected in a zonal direction. At the same time, over the eastern Atlantic, the intensification of the STJ traps the air masses transporting the water vapor around the globe, maintaining wet air masses in the jet.

The wind field at 200 hPa (~12.5 km) on 1 June 2007 (Figure 6a), shows a pronounced jet around at the 25–35° S latitude band, mainly over South America (with anomalies on its eastern part), in Africa, and in the middle of the Indian Ocean at the latitude of India. In those three areas, the jet was deflected into two parts: a weak one towards the north, reconnecting the jet afterward, and a stronger branch reconnecting the jet after a large southern loop. Such synoptic context is similar to the situation of the multiple stratospheric intrusion events in April 2013 above the Indian Ocean, where some isentropic transport was associated with Rossby wave breakings guided by both subtropical and polar jet streams [33].

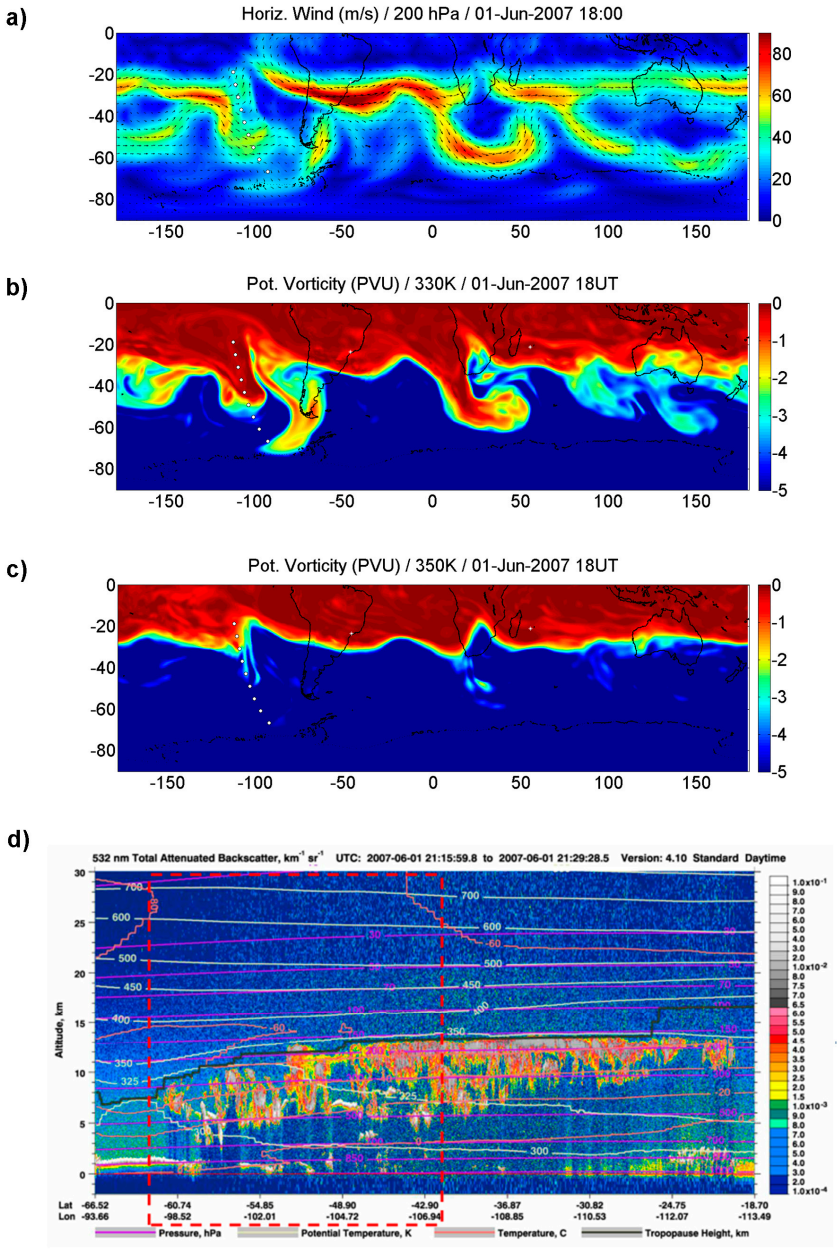

Figure 6. (**a**) Wind map at 200 hPa for 1 June 2007 by ECMWF-ERA-Interim reanalysis. Arrows indicate the direction, while colors indicate the wind intensity in m s^{-1}. (**b**) Advected potential vorticity (PV) field at 330 K by LACYTRAJ at 18 UTC on 1 June 2007. (**c**) Advected PV field at 350 K by LACYTRAJ at 18 UTC on 1 June 2007. (**d**) CALIPSO cloud detection, 21:15 to 21:29 UTC on 1 June 2007. The white dot lines in (**b**) and (**c**) indicate the CALIPSO tracking shown in (**d**). The white stars in (**b**) and (**c**) indicate the cirrus cloud detection by MSP and Maïdo lidars.

The ECMWF ERA-Interim potential vorticity (PV) field at the altitude of the cirrus cloud on 1 June 2007 between the potential temperature level of 330 and 350 K (Figure 5), provided by the LACYTRAJ model (Figure 6b,c), reveals that when the jet is deflected abruptly, filaments of tropical air are generated that may lead to irreversible transport. CALIPSO observations extracted around these filament structures clearly reveal the presence of ice crystals. 350 K corresponds to the tropopause over 30° S, while 330 K corresponds to the tropopause around 56° S. A portion of clouds was observed above the tropopause at around 50° S, in agreement with PV fields as observed in Figure 6d. Such a transport is isentropic, and due here to isentropic surfaces that cross the tropopause in opposition to potential overshooting effects. Similar processes have been identified and described in the northern hemisphere at mid-latitude [34]. This is a key process for hydrating the stratosphere. Water is then also removed from the jet, which is full of moisture from the equatorial convection regions (as illustrated in Figure 3), even if a small portion of ice is concerned.

4. CALIPSO Cloud Signature and Tracking of Air Masses

The solid phase is easy to detect using lidar, due to the high scattering effects by crystals. In this case, cirrus clouds detection has been used as a proxy for enhanced water vapor density, despite temperature and local dynamics that may interfere in the life cloud cycle.

The cirrus case reported on 1 June 2007and detected by MSP-lidar (Figure 1) was analyzed, and the respective altitudes of the cloud base, mean height, and top of cirrus (14, 15, and 16 km) were used as the critical levels and starting point of the LACYTRAJ forward trajectories. LACYTRAJ simulated many trajectories with a small dispersion, to account for the trajectory mean (colored solid lines in Figure 7). The colored bands in Figure 7 represent the upper and lower limits determined by LACYTRAJ, according to the standard deviation for each variable (Figure 7).

These shapes of trajectories were used to identify cloud occurrences within the CALIPSO coincidences. The CALIPSO data throughout the region close to the coordinates of the forward trajectories (taking into account the band limits for each variable) were selected and superimposed on the LACYTRAJ trajectories in Figure 7. On 1 June 2007, when MSP-lidar was observed, a cloud was detected by CALIPSO in the same range of altitude and latitude. The air mass temperatures showed some large evolutions (10–20 K) depending of the altitude considered. Temperature evolution provided by CALIPSO cloud temperature and LACYTRAJ exhibited a similar evolution (Figure 7).

For the following days, good agreements were obtained, up to 3 June 2007, when trajectories were shifting southward and spreading on a large latitudinal domain, air masses descended by 1–2 km, and temperature increased by 15 to 30 K. A cirrus cloud on 3 June was not observed by CALIPSO, with temperatures between 215 and 230 K. On 4–5 June 2007, trajectories returned to the Equator as they remained on the same isentropic level, temperatures cooled back to the same level, and cirrus clouds were then detected again, mainly for the trajectory corresponding to the mean altitude of the initial cloud observed above São Paulo. Some layers were inverted after the fifth day, followed also by temperature inversion. The standard deviation of the modeled curves becomes higher. A possible explanation for this increase of the standard deviation after 5 June could be the vertical dispersion of air masses during the transport, shown by the color of the trajectory points in Figure 4. Between 1 and 4 June 2007, the particle cluster was confined to an atmospheric layer of fairly small thickness. All points of trajectory points were around 12 km. However, after 5 June 2007, the north–south horizontal dispersion was quite small, because the air masses were following the jet stream, but the vertical dispersion of the trajectory points increased. On 5 June 2007, above the Indian Ocean, the trajectory points were between 13.5 km and 14.5 km, and on 6 June, above Australia, they were between 12 and 15 km. The spread in latitude remained large up to 8 June, when the trajectories arrived in the middle of the Pacific. The trajectory corresponding to the upper part of the initial cloud was going quite south with warmer temperature up to 8 June. No cirrus cloud was observed by CALIPSO at this location.

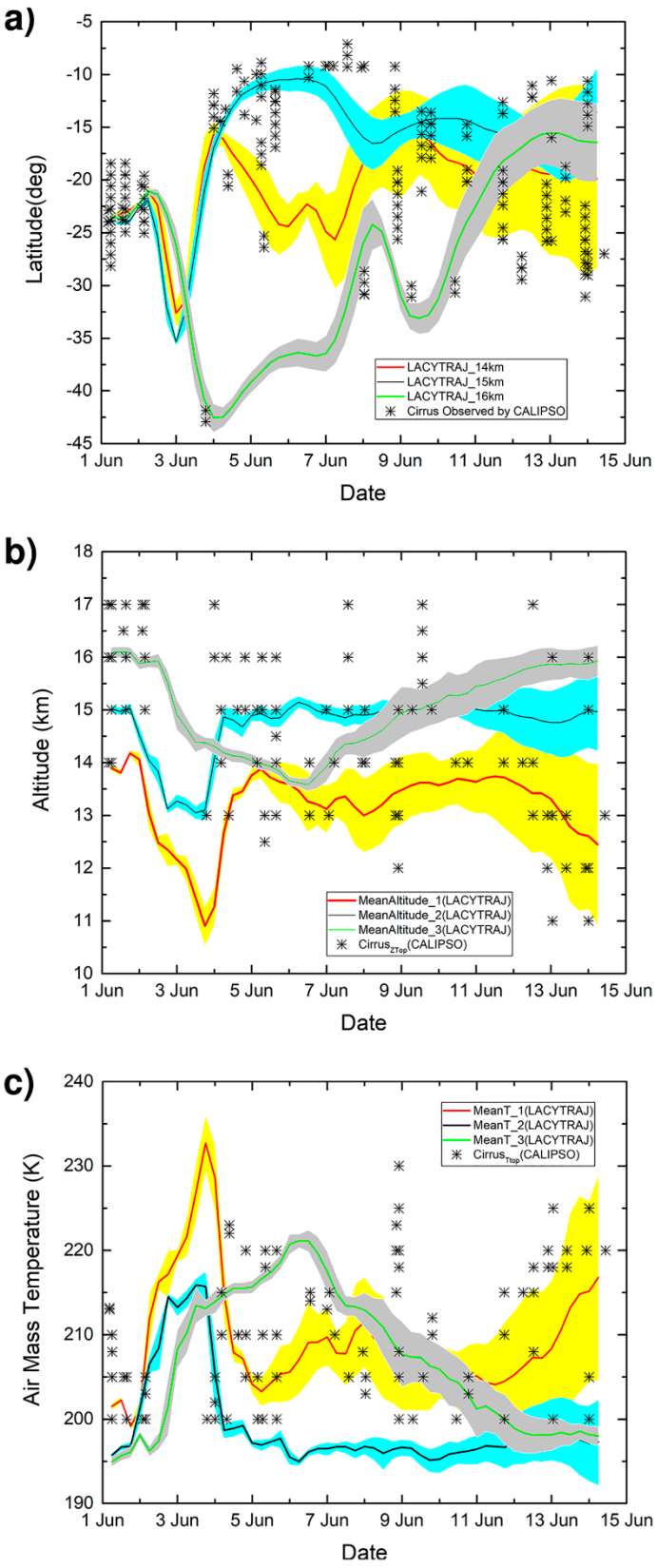

Figure 7. Track matching between CALIPSO (presence of cirrus detected) and LACYTRAJ air mass trajectories during 14 days in a latitude range of −45° to −5°. The corresponding latitude (**a**), altitude (**b**), and temperature (**c**) of cirrus extracted from CALIPSO are shown for the same period. The shaded area on the modeled curves represents the standard deviation.

At that time, a few trajectories (Figure 4) were going more to the north and then were lifted up and turned for several days (10–14 June 2007), up to 15–16 km, while the rest of the trajectory groups flew over São Paulo again on 12 June. For the trajectories going up, CALIPSO revealed the presence of very high clouds with a low temperature of 200 K (Figure 8).

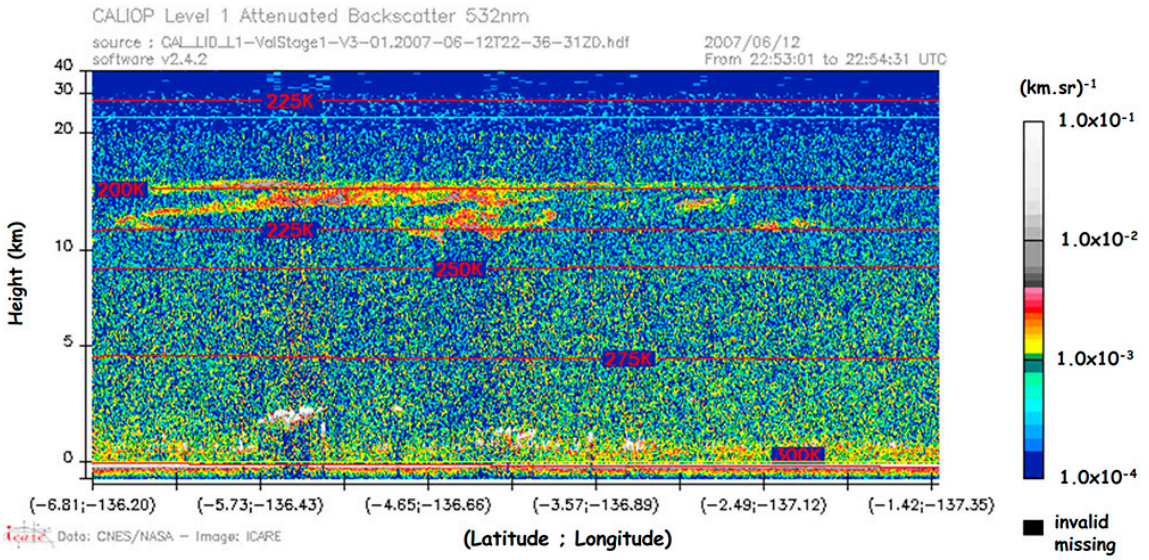

Figure 8. Cirrus anvil observed by CALIOP.

5. Estimating Ice Crystal Sedimentation

This study shows that the lifetime of a wet air mass possibly associated with cirrus cloud occurrence could be as long as 12 days. Thanks to the CALIPSO observations, the presence of the ice phase can be checked and monitored regularly. The CALIOP measurements show that clouds existed when the CALIPSO footprints crossed LACYTRAJ trajectories (Figure 7a), except on 3–4 June, when the trajectories moved south, at a lower altitude with warmer temperatures. The spatiotemporal coincidences were not perfect, and could have induced temperature uncertainties of several Kelvins. However, such cirrus clouds extend over an area of several hundred km (Figure 3b) and have been observed over São Paulo for several hours confirming that a large extension and then non-perfect coincidence should not be an issue.

After 12 days, the cirrus was 2–3 km lower in altitude compared to its initial altitude of detection by the MSP-lidar on 1 June 2007. The trajectories reveal that the air masses remained on the same isentropic level with a vertical spread after 12 days of ±10 Kelvins. If we consider the cloud altitudes from 1–12 June according to the potential temperature, a shift of 20–40 K can be observed, showing that a real decrease in temperature occurred. The transport of ice crystals in the upper troposphere may have differed from the trajectory estimates due to sedimentation induced by the particle gravity [35,36].

Following the Match technique, adopted to estimate crystal mean fall speed [15], we could estimate a mean sedimentation (S) of 0.1–0.2 cm s^{-1} for this selected case, with an uncertainty of 0.05 cm s^{-1} according to the divergence of trajectories. Even if this estimate is characterized by a large uncertainty [15], the derived value of S around the 14–16 km altitude region was lower than what we expected for sub-visible clouds [37].

6. Conclusions

From all the measurements performed by the MSP-lidar, one case (1 June 2007) has been chosen for this study (Figure 1), due to its representativeness of the type of cirrus clouds and their origin before being observed over São Paulo and detected by the lidar system, as well as to test the Lagrangian approach. This case is also interesting for investigating a sub-tropical cirrus lifetime when air masses

are trapped by the STJ around the globe, as air masses were passed again above São Paulo on 12 June 2007, and cirrus was detected again by the MSP-lidar (Figure 3.)

In this work, we have investigated a case of a cirrus cloud doing a full planet rotation following the STJ and passing over the same place twice. As already reported [13], the lidar at São Paulo observed a cirrus cloud coming from the jet, but also from air masses coming from convection regions present in the Equator that brought the humidity for anvil cirrus cloud formation, and these air masses going south were mixed with those coming from South Pacific Ocean by STJ. This case illustrates that water vapor is channelized by the jet, providing a large cloud occurrence in the upper troposphere. In this case, the jet stream presented some anomalies that deflected to the south the trajectory, leading to warmer temperatures. The cloud disappears (near the African continent on 3 June 2007 in this case), which is probably associated with a stratospheric intrusion and simultaneously experiencing a colder temperature. Such anomalies can generate filamentary structures that potentially inject water at mid-latitudes, as well as crystals directly into the stratosphere, as reported in the northern hemisphere by Montoux et al. [34]. This can be considered as a water vapor sink in the tropical jet, while the main source is the equatorial convection.

Observations of the same air masses with the same lidar after 12 days exhibit a sedimentation estimate of 0.1–0.2 cm s^{-1}, which is very small and probably due to sub-visible clouds forming at the upper tropical tropopause around the 14–16 km altitude region, and exhibiting crystals with smaller sizes. These small sizes could explain such a small sedimentation and the large water vapor density remaining trapped by the jet for weeks.

However, such a Lagrangian study does not allow accurate microphysical study to be addressed. One reason is the missing information about air water density. The second one is associated with the too-small number of accurate spatiotemporal coincidences between CALIOP observations and the cirrus trajectory. Better sampling with more lidar in space would be required to better understand water transport at the vicinity of the tropopause. In the near future, such Lagrangian approach should take benefit to stratospheric balloons with onboard lidar as well as temperature and water measurements, such as those planned to be launched through the balloon experiment called Strateole 2 being prepared by the French space agency CNES [14]. This study is then useful for the preparation of the flying plans of future balloon campaigns.

Author Contributions: Conceptualization: P.K. and E.G.L.; methodology: P.K., E.G.L., J.-L.B., and W.M.N.; software: E.G.L., W.M.N., P.K., and J.-L.B.; validation: E.G.L., P.K., J.-L.B., W.M.N., D.D., and H.V.; investigation: E.G.L., P.K., J.-L.B., W.M.N., H.V., D.D., E.L., S.K., and F.R.; resources: P.K. and E.L., data curation: P.K. and E.L., writing (original draft preparation): E.G.L., P.K., J.-L.B., and W.M.N.; writing (review and editing): E.G.L., P.K., J.-L.B., H.V., W.M.N., and D.D.; supervision: P.K.; project administration: P.K.; funding acquisition: P.K.

Funding: This research was funded by Comissão Nacional de Energia Nuclear (CNEN/IPEN) and the Conselho Nacional de Desenvolvimento Científico e Tecnológico (CNPq) grant number 150760/2012-4, Brazilian government.

Acknowledgments: The CALIOP data were made available at the ASDC data ordering (https://www-calipso.larc.nasa.gov/) and ICARE data center (http://www-icare.univ-lille.fr). We acknowledge Bertrand Cadet and Denis Faduilhe for operating lidar measurement, Sandra Banson-Valleix for the ECMWF ERA-Interim theta profile, and Francoise Posny as PI in charge of radiosonde database at La Réunion during this case study. The measurements of MSP lidar were performed by the lidar group at the Center for Laser and Applications (CLA/IPEN/Brazil). The radiosonde used to determine MSP and La Réunion lidar profiles were extracted at the Wyoming University database (http://weather.uwyo.edu/upperair/sounding.html) and SHADOZ database (http://croc.gsfc.nasa.gov/shadoz/), respectively.

Conflicts of Interest: The authors declare no conflict of interest.

References

1. Forster, P.M.; Shine, K.P. Assessing the climate impact of trends in stratospheric water vapor. *Geophys. Res. Lett.* **2002**, *29*, 1086. [CrossRef]
2. Jensen, E.J.; Toon, O.G.; Westphal, D.L.; Kinne, S.; Heymsfield, A.J. Mycrophysical modelling of cirrus. Part I: Comparison with 1986 FIRE IFO measurements. *J. Geophys. Res.* **1994**, *99*, 10421–10442. [CrossRef]

3. Homeyer, C.R.; Pan, L.L.; Dorsi, S.W.; Avallone, L.M.; Weinheimer, A.J.; O'Brien, A.S.; DiGangi, J.P.; Zondlo, M.A.; Ryerson, T.B.; Diskin, G.S.; et al. Convective transport of water vapor into the lower stratosphere observed during double-tropopause events. *J. Geophys. Res. Atmos.* **2014**, *119*, 10941–10958. [CrossRef]
4. Fujita, T.T. Principle of stereoscopic height computations and their applications to stratospheric cirrus over severe thunderstorms. *J. Meteorol. Soc. Jpn.* **1982**, *60*, 355–368. [CrossRef]
5. Adler, R.F.; Markus, M.J.; Fenn, D.D.; Szejwach, G.; Shenk, W.E. Thunderstorm top structure observed by aircraft overflights with an infrared radiometer. *J. Clim. Appl. Meteorol.* **1983**, *22*, 579–593. [CrossRef]
6. Levizzani, V.; Setvák, M. Multispectral, high-resolution satellite observations of plumes on top of convective storms. *J. Atmos. Sci.* **1996**, *53*, 361–369. [CrossRef]
7. Wang, P.K. Moisture plumes above thunderstorm anvils and their contributions to cross-tropopause transport of water vapor in midlatitudes. *J. Geophys. Res.* **2003**, *108*, 4194. [CrossRef]
8. Fueglistaler, S.; Dessler, A.E.; Dunkerton, T.J.; Folkins, I.; Fu, Q.; Mote, P.W. Tropical tropopause layer. *Rev. Geophys.* **2009**, *47*, RG1004. [CrossRef]
9. Pommereau, J.-P.; Garnier, A.; Held, G.; Gomes, A.M.; Goutail, F.; Durry, G.; Borchi, F.; Hauchecorne, A.; Montoux, N.; Cocquerez, P.; et al. An overview of the HIBISCUS campaign. *Atmos. Chem. Phys.* **2011**, *11*, 2309–2339. [CrossRef]
10. Wielicki, B.A.; Wong, T.M.; Allan, R.P.; Slingo, A.; Kiehl, J.T.; Soden, B.J.; Gordon, C.T.; Miller, A.J.; Yang, S.K.; Randall, D.A.; et al. Evidence for large decadal variability in the tropical mean radiative energy budget. *Science* **2002**, *295*, 841–844. [CrossRef] [PubMed]
11. Comstock, J.M.; Jakob, C. Evaluation of tropical cirrus cloud properties derived from ECMWF model output and ground-based measurements over Nauru Island. *Geophys. Res. Lett.* **2004**, *31*, L10106. [CrossRef]
12. Mitchell, D.L.; Rasch, P.; Ivanova, D.; McFarquhar, G.; Nousiainen, T. Impact of small ice crystal assumptions on ice sedimentation rates in cirrus clouds and GCM simulations. *Geophys. Res. Lett.* **2008**, *35*, L09806. [CrossRef]
13. Larroza, E.G.; Nakaema, W.M.; Bourayou, R.; Hoareau, C.; Landulfo, E.; Keckhut, P. Towards an automatic lidar cirrus cloud retrieval for climate studies. *Atmos. Meas. Tech.* **2013**, *6*, 3197–3210. [CrossRef]
14. Haase, J.S.; Alexander, M.J.; Hertzog, A.; Kalnais, L.; Deshler, T.; Davis, S.M.; Plougonyen, R.; Cocquerez, P.; Venel, S. *Around the World in 84 Days*; Eos; Collector's Guide Publishing: Burlington, MA, USA, 2018; p. 99.
15. Dionisi, D.; Keckhut, P.; Hoareau, C.; Montoux, N.; Congeduti, F. Cirrus crystal fall velocity estimated using the match method with ground-based lidars: A first case study. *Atmos. Meas. Tech.* **2013**, *6*, 457–470. [CrossRef]
16. Landulfo, E.; Papayannis, A.; Artaxo, P.; Castanho, A.D.A.; de Freitas, A.Z.; Souza, R.F.; Vieira Junior, N.D.; Jorge, M.P.; S'anchez-Ccoyllo, O.R.; Moreira, D.S. Synergetic measurements of aerosols over São Paulo, Brazil using LIDAR, sunphotometer and satellite data during dry season. *Atmos. Chem. Phys.* **2003**, *5*, 1523–1539. [CrossRef]
17. Baray, J.-L.; Leveau, J.; Baldy, S.; Jouzel, J.; Keckhut, P.; Bergametti, G.; Ancellet, G.; Bencherif, H.; Cadet, B.; Carleer, M.; et al. An instrumented station for the survey of ozone and climate change in the southern tropics: Scientific motivation, technical description and future plans. *J. Environ. Monit.* **2006**, *8*, 1–9. [CrossRef]
18. Cadet, B.; Goldfarb, L.; Faduilhe, D.; Baldy, S.; Giraud, V.; Keckhut, P.; Rechou, A. A sub-tropical cirrus cloud climatology from Reunion island (21° S, 66° E) lidar data set. *Geophys. Res. Lett.* **2003**, *30*, 1130. [CrossRef]
19. Baray, J.-L.; Courcoux, Y.; Keckhut, P.; Portafaix, T.; Tulet, P.; Cammas, J.-P.; Hauchecorne, A.; Beekmann, S.G.; De Mazière, M.; Hermans, C.; et al. Maïdo observatory: A new high-altitude station facility at Reunion Island (21° S, 55° E) for long-term atmospheric remote sensing and in situ measurements. *Atmos. Meas. Tech.* **2013**, *6*, 2865–2877. [CrossRef]
20. Bucholtz, A. Rayleigh-scattering calculations for the terrestrial atmosphere. *Appl. Opt.* **1995**, *34*, 2765–2773. [CrossRef] [PubMed]
21. Garnier, A.; Pelon, J.; Dubuisson, P.; Faivre, M.; Chomette, O.; Pascal, N.; Kratz, D.P. Retrieval of cloud properties using CALIPSO Imaging Infrared Radiometer. Part I: Effective emissivity and optical depth. *J. Appl. Meteorol. Climatol.* **2012**, *51*, 1407–1425. [CrossRef]
22. Vaughan, M.A.; Winker, D.M.; Powell, K.A. Fully automated detection of cloud and aerosol layer in the CALIPSO lidar measurements. *J. Atmos. Ocean. Technol.* **2009**, *26*, 2034–2050. [CrossRef]

23. Fu, Y.; Chen, Y.; Li, R.; Qin, F.; Xian, T.; Yu, L.; Zhang, A.; Liu, G.; Zhang, X. Lateral Boundary of Cirrus Cloud from CALIPSO Observations. *Nat. Sci. Rep.* **2017**, *7*, 14221. [CrossRef] [PubMed]
24. Liu, Z.; Omar, A.H.; Hu, Y.; Vaughan, M.A.; Winker, D.M. The CALIPSO lidar cloud and aerosol discrimination: Version 2 algorithm and initial assessment of performance. *J. Atmos. Ocean. Technol.* **2009**, *26*, 1198–1213. [CrossRef]
25. Anselmo, T.; Clifton, R.; Hunt, W.; Lee, K.-P.; Murray, T.; Powell, K.; Rodier, S.D.; Vaughan, M.; Chomette, O.; Viollier, M.; et al. *Cloud-Aerosol LIDAR Infrared Pathfinder Satellite Observations Data Management System and Data Product Catalog*; CALIPSO Algorithm Theoretical Basis Document, Document No: PC-SCI-503; National Aeronautics and Space Administration Langley Research Center: Hampton, VA, USA, 2007; p. 100.
26. Clain, G.; Baray, J.-L.; Delmas, R.; Keckhut, P.; Cammas, J.-P. A lagrangian approach to analyse the tropospheric ozone climatology in the tropics: Climatology of Stratosphere—Troposphere exchange at Reunion Island. *Atmos. Environ.* **2010**, *44*, 968–975. [CrossRef]
27. Dee, D.P.; Uppala, S.M.; Simmons, A.J.; Berrisford, P.; Poli, P.; Kobayashi, S.; Andrae, U.; Balmaseda, M.A.; Balsamo, G.; Bauer, D.P.; et al. The ERA-Interim reanalysis: Configuration and performance of the data assimilation system. *Q. J. R. Meteorol. Soc.* **2011**, *137*, 553–597. [CrossRef]
28. Zimmermann, D.F.R. Subtropical Jet Climatology over South America. Master's Thesis, University of São Paulo, São Paulo, Brazil, 2017.
29. Escobar, G. Jatos de Altos Níveis. In *Tempo e Clima no Brasil*; de Cavalcanti, I.F.A., Ferreira, N.J., da Silva, M.G.A.J., Dias, M.A.F.S., Eds.; Oficina de Textos: São Paulo, Brazil, 2009; pp. 127–134, ISBN 978-85-86238-92-5.
30. Thompson, D.W.J.; Wallace, J.M. Annular Modes in the Extratropical Circulation. Part I: Month-to-Month Variability. *J. Clim.* **1999**, *13*, 1000–1016. [CrossRef]
31. Sassen, K.; Wang, Z. Classifying clouds around the globe with the CloudSat radar: 1-year of results. *Geophys. Res. Lett.* **2008**, *35*, L04805. [CrossRef]
32. Sassen, K.; Wang, Z.E.; Liu, D. Cirrus clouds a deep convection in the tropics: Insights from CALIPSO and CloudSat. *J. Geophys. Res.* **2009**, *114*, D00H06. [CrossRef]
33. Vérèmes, H.; Cammas, J.-P.; Baray, J.-L.; Keckhut, P.; Barthe, C.; Posny, F.; Tulet, P.; Dionisi, D.; Bielli, S. Multiple subtropical stratospheric intrusions over Reunion Island: Observational, lagrangian, and eulerian numerical modeling approaches. *J. Geophys. Res. Atmos.* **2016**, *121*, 14414–14432. [CrossRef]
34. Montoux, N.; Keckhut, P.; Hauchecorne, A.; Jumelet, J.; Brogniez, H.; David, C. Isentropic modeling of a cirrus cloud event observed in the midlatitude upper troposphere and lower stratosphere. *J. Geophys. Res.* **2010**, *115*, D02202. [CrossRef]
35. Starr, D.O.C.; Cox, S.K. Cirrus Clouds, Part I: A Cirrus Cloud Model. *Am. Meteorol. Soc.* **1985**, *42*, 2663–2681. [CrossRef]
36. Spichtinger, P.; Gierens, K.; Lohmann, U. Importance of a proper treatment of ice crystal sedimentation for cirrus clouds in large-scale models. In Proceedings of the AMS 12th Cloud Physics, Madison, WI, USA, 10–14 July 2006.
37. Karcher, B. Properties of subvisible cirrus clouds formed by homogeneous freezing. *Atmos. Chem. Phys.* **2002**, *2*, 161–170.